Geophys. J. Int. (2008) **174,** 1–13 doi: 10.1111/j.1365-246X.2008.03803.x

Three-dimensional gravity inversion for Moho depth at rifted continental margins incorporating a lithosphere thermal gravity anomaly correction

A. R. Chappell and N. J. Kusznir

University of Liverpool, Department of Earth & Ocean Sciences, Jane Herdman Laboratories, 4 *Brownlow Street, Liverpool* L69 3GP, *UK.*
E-mail: alex_chappell@hotmail.com

Accepted 2008 March 19. Received 2008 March 18; in original form 2007 May 10

SUMMARY

This paper describes a method for determining Moho depth, lithosphere thinning factor ($\gamma = 1 - 1/\beta$) and the location of the ocean–continent transition at rifted continental margins using 3-D gravity inversion which includes a correction for the large negative lithosphere thermal gravity anomaly within continental margin lithosphere. The lateral density changes caused by the elevated geotherm in thinned continental margin and adjacent ocean basin lithosphere produce a significant lithosphere thermal gravity anomaly which may be in excess of −100 mGal, and for which a correction must be made in order to determine Moho depth accurately from gravity inversion. We describe a method of iteratively calculating the lithosphere thermal gravity anomaly using a lithosphere thermal model to give the present-day temperature field from which we calculate the lithosphere thermal density and gravity anomalies. For continental margin lithosphere, the lithosphere thermal perturbation is calculated from the lithosphere thinning factor ($\gamma = 1 - 1/\beta$) obtained from crustal thinning determined by gravity inversion and breakup age for thermal re-equilibration time. For oceanic lithosphere, the lithosphere thermal model used to predict the lithosphere thermal gravity anomaly may be conditioned using ocean isochrons from plate reconstruction models to provide the age and location of oceanic lithosphere. A correction is made for crustal melt addition due to decompression melting during continental breakup and seafloor spreading. We investigate the sensitivity of the lithosphere thermal gravity anomaly and the predicted Moho depth from gravity inversion at continental rifted margins to the methods used to calculate and condition the lithosphere thermal model using both synthetic models and examples from the North Atlantic.

Key words: Inverse theory; Gravity anomalies and Earth structure; Continental margins: divergent; Crustal structure.

1 INTRODUCTION

The determination of Moho depth, crustal thickness and thinning factor ($\gamma = 1 - 1/\beta$) is important at rifted continental margins for understanding the structure and location of the ocean–continent transition (OCT). In this paper, we describe a 3-D gravity inverse method to predict Moho depth at rifted continental margins which corrects for the significant lithosphere thermal gravity anomaly due to the lateral changes in lithosphere temperature and density that occur in the transition from unthinned continental to oceanic lithosphere.

Extending and thinning continental lithosphere, leading to breakup and the formation of oceanic lithosphere, results in a steepened geotherm, which subsequently relaxes towards an equilibrium gradient as the lithosphere cools. The lateral changes in lithosphere density that result from the perturbed geotherm produce a large thermal gravity anomaly (Fig. 1) (Louden & Forsyth 1976; Cochran & Talwani 1977; Watts *et al.* 1985; Kuo & Forsyth 1989; Crosby *et al.* 2006), which may reach −320 mGal in new oceanic lithosphere and remains large at rifted continental margins (Karner & Watts 1982; Breivik *et al.* 1999; Kimbell 2004).

In oceanic lithosphere, we can estimate the geotherm and the lithosphere thermal gravity anomaly from *a priori* information, since the temperature of the lithosphere is solely dependent on age. To achieve this, we use a thermal model of the lithosphere (McKenzie 1978) conditioned by ocean isochron ages (e.g. Müller *et al.* 1997).

In rifted continental margin lithosphere, the present temperature of the margin lithosphere is dependent on age and the magnitude of lithosphere thinning. We use breakup age as the age estimate; however, we do not know the lithosphere thinning-factor distribution used to estimate the initial perturbation of the geotherm from *a priori* information. To overcome this, we use an iterative solution to determine lithosphere thinning, the geotherm perturbation and

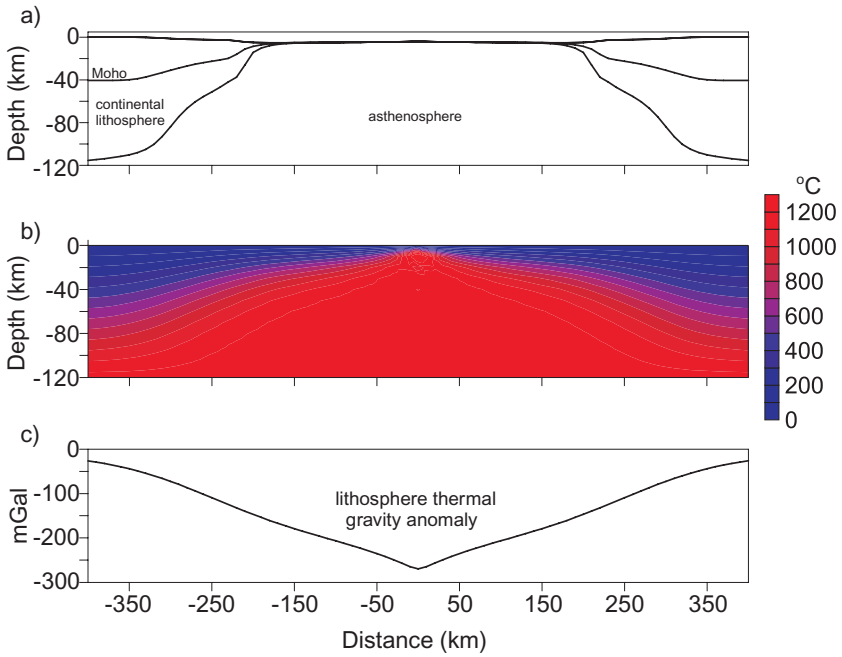

Figure 1. (a) Lithosphere cross-section through a model of continental breakup and seafloor spreading at 20 Myr after breakup. (b) The associated temperature field at 20 Myr showing the large lateral changes in lithosphere temperature which generate the lithosphere thermal gravity anomaly. (c) The lithosphere thermal gravity anomaly produced by the above model is very large at the ocean ridge and still substantial (>100 mGal) for the rifted continental margin.

the lithosphere thermal gravity anomaly. Initially we invert the mantle residual gravity anomaly for Moho depth without a correction for the lithosphere thermal gravity anomaly and estimate the lithosphere thinning factor from the crustal thickness prediction. We then calculate the temperature field (McKenzie 1978) and the initial lithosphere thermal gravity anomaly, which we subtract from the mantle residual gravity anomaly. The inversion is subsequently a recursive cycle of inverting for Moho depth, calculating the lithosphere thermal gravity anomaly and updating the mantle residual gravity anomaly until convergence is achieved (Fig. 2).

To calculate the lithosphere thinning-factor from the crustal thinning factor we assume that the lithosphere deforms by pure shear and assume that crustal thinning and lithosphere thinning are equal. Additionally a correction is made to continental crustal basement thickness for melt addition during continental breakup using the models of McKenzie & Bickle (1988) and White & McKenzie (1989) conditioned by a mantle potential temperature appropriate to the margin of interest to predict the thickness of melt addition. We assume that all melt generated by decompression melting during thinning and extension of continental lithosphere contributes to the observed crustal thickness.

Using gravity inversion to predict Moho depths in agreement with seismic observations depends on accurate sediment thickness and oceanic lithosphere age data being available; however, the method

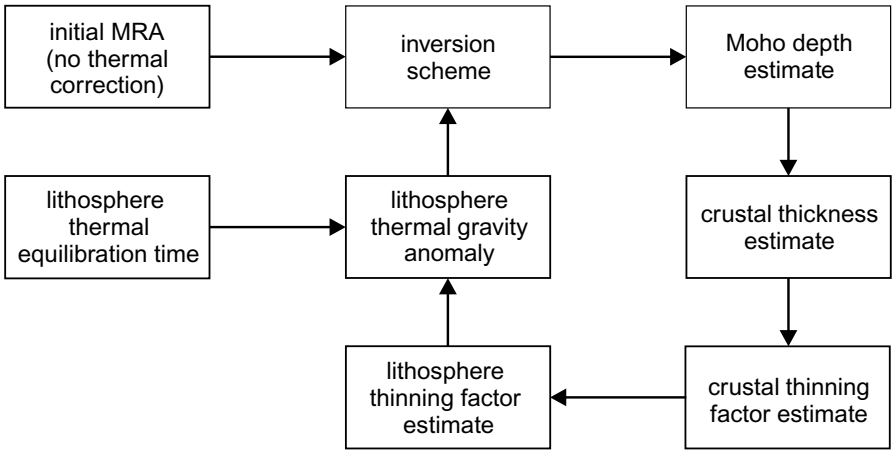

Figure 2. The gravity inversion workflow for determining Moho depth incorporating an iterative solution for the lithosphere thermal gravity anomaly. The initial mantle residual anomaly is inverted for Moho depth and the lithosphere thinning factor is derived. This, in addition to lithosphere equilibration times from break up age and/or ocean isochrons, conditions a lithosphere thermal model from which the lithosphere thermal gravity anomaly is calculated. The lithosphere thermal gravity anomaly is then subtracted from the initial mantle residual gravity anomaly and the inversion process repeated until numerical convergence is achieved.

can still give useful results where this data is absent. Without a correction for sediment thickness to the mantle residual anomaly, the inversion method produces maximum bounds of Moho depth and crustal thickness and minimum bounds of lithosphere thinning factor and lithosphere thermal gravity anomaly. For situations where isochrons do not accurately represent the age or location of the OCT or the age of oceanic lithosphere, we show that we can use the melt-corrected thinning factor to estimate the position of the OCT and avoid introducing potentially large errors.

We apply the gravity inversion method to examples from the North Atlantic rifted margins in order to demonstrate the necessity of correcting for the lithosphere thermal gravity anomaly and examine alternate methods of conditioning the thermal model at continental margins.

2 METHOD

We recognize that there are two approaches to using gravity to predict Moho depth. First, inverting directly for Moho depth if we can overcome the problem of non-uniqueness and secondly, using a process-based approach in which we use a geodynamic model to predict a gravity anomaly that we compare to observed gravity and adjust to minimize a misfit function (e.g. Watts & Fairhead 1999; Kimbell *et al.* 2004). In this paper, we adopt the first approach. Smith (1961) provides a set of conditions that allow an anomaly and a source distribution to be uniquely associated; he shows that the density of the source must be constant, it must be of finite extent and any vertical line must pass through the body no more than once. This requires that the Moho surface we invert for must be single-valued and the density of crust and mantle must be constant.

2.1 Gravity inversion

The gravity anomaly due to lateral changes in Moho depth is the mantle residual anomaly. The free air gravity anomaly as the sum of the major components is

$$g_{\mathrm{faa}} = g_{\mathrm{mra}} + g_{\mathrm{b}} + g_{\mathrm{t}} + g_{\mathrm{s}}, \tag{1}$$

where g_{faa} is the free air anomaly, g_{mra} is the mantle residual anomaly arising from variation in Moho depth, g_{b} is the anomaly from lateral changes in bathymetry or topography, g_{t} is the lithosphere thermal gravity anomaly and g_{s} is the gravity anomaly due to changes in sediment thickness and density. We rearrange to isolate the mantle residual

$$g_{\mathrm{mra}} = g_{\mathrm{faa}} - g_{\mathrm{b}} - g_{\mathrm{t}} - g_{\mathrm{s}}. \tag{2}$$

In this paper, we use the Sandwell & Smith (1997) satellite altimetry gravity data for g_{faa}. We calculate g_{b} from the an independent bathymetry and topography compilation (IOC 2003) using the method of Parker (1972),

$$F\left[\Delta g\right] = -2\pi G e^{-|k|z} \sum_{n=1}^{\infty} \frac{|k|^{n-1}}{n!} F[\Delta\rho(x,y)h(x,y)^n], \tag{3}$$

where F[] represents a 2-D discrete Fourier transform, Δg the gravity anomaly, G the universal gravitational constant (6.672×10^{-11} Nm^2 kg^{-2}), $\Delta\rho(x,y)$ the density contrast of the body; $h(x,y)$ is topography measured from a plane at depth z below the observation plane and $|k|$ is the absolute value of the wave vector. Axes are orientated with z positive upwards. We calculate the lithosphere thermal gravity anomaly, g_{t}, iteratively (Section 2.2). If we assume that $g_{\mathrm{s}} = 0$, we produce a maximum bound of Moho depth. If we can estimate g_{s}, we can predict a more accurate Moho depth that can be compared to wide-angle seismic results. Where we have accurate sediment thickness and density data, we calculate g_{s} using the method of Chappell & Kusznir (2008b). To simplify interpretation, we prefer to assume $g_{\mathrm{s}} = 0$ rather than use inconsistent regional sediment maps compiled from many sources. If profile data is available from seismic lines, we interpolate sediment thickness into map form, invert for Moho depth in 3-D and then confine our interpretation to the original lines, where sediment thickness is constrained.

A number of inversion methods exist to calculate the topography of the Moho surface from the mantle residual gravity anomaly (e.g. Bott 1960; Cordell & Henderson 1968; Oldenburg 1974; Granser 1987). We typically use either the wavenumber domain method described by Oldenburg (1974),

$$F[h(x,y)] = -\frac{F[\Delta g(x,y)]e^{|k|z}}{2\pi G\rho} - \sum_{n=2}^{\infty} \frac{|k|^{n-1}}{n!} F[h(x,y)^n], \tag{4}$$

or a modification of the Bott (1960) method similar to the approach of Cordell & Henderson (1968) and Greenhalgh & Kusznir (2007) utilizing eq. (3) to calculate the gravity anomaly on a regular grid. Convergence of the Oldenburg (1974) method depends on the frequency content of the gravity data, the reference datum (z) depth and filter parameters. Generally, we find that convergence is rapid, even when the data is not in the region of guaranteed convergence calculated by Granser (1986). If the Oldenburg (1974) method fails to converge, we use the slower method of Bott (1960), utilizing the forward gravity algorithm (eq. 3). In order for eq. (4) to converge, we filter the mantle residual anomaly using a zero-bounded low-pass filter of the form suggested by Oldenburg (1974). This removes short wavelength anomalies, caused by shallow sources within the crust, which are not due to Moho topography. Appropriate cut-off values for Moho inversion with this form of filter (Oldenburg 1974) are 75 and 150 km. If we use the Bott (1960) method, we use a Butterworth filter (e.g. Sheriff & Geldart 1999) with 100 km wavelength and $n = 2$ to produce comparable results.

To satisfy Smith's (1961) theorem, we must use constant crust and mantle densities. For the mantle we use 3330 kg m^{-3} since we are calculating the lithosphere thermal gravity anomaly relative to that value (McKenzie 1978) and it is within the restricted range of densities suggested by the composition of mantle rocks (Poudjom Djomani *et al.* 2001). Studies show that the mean densities of both continental and oceanic crust are close to 2850 kg m^{-3} (Carlson & Herrick 1990; Christensen & Mooney 1995). By adopting this assumption in the gravity inversion, we expect that our Moho depth prediction will tend to be shallower than observations in regions of relatively dense crust and deeper than observations in regions of relatively light crust.

2.2 Lithosphere thermal gravity anomaly

To estimate the lithosphere temperature and density perturbations from which we calculate the lithosphere thermal gravity anomaly, we calculate an estimate of the temperature field using a cooling-plate model (McKenzie 1978). We use this model because it is a fast analytical solution and we require temperature calculations at ~6.6 $\times 10^6$ points when we are using a typical 512 $\times$ 512 grid and 5 km vertical spacing. The temperature anomaly in °C, T_z, at depth z is

given by

$$T_z = \frac{2T_m}{\pi}\sum_{n=1}^{\infty}\frac{(-1)^{n+1}}{n}\left[\frac{\beta}{n\pi}\sin\left(\frac{n\pi}{\beta}\right)\right] \times \exp\left(\frac{-n^2 t}{\tau}\right)\sin\left(\frac{n\pi z}{a}\right), \quad (5)$$

in which T_m is base-lithosphere temperature; β is the lithosphere stretching-factor (McKenzie 1978) equal to equilibrium lithosphere thickness divided by the initial thinned lithosphere thickness; τ is the lithosphere cooling thermal decay constant and a is equilibrium lithosphere (plate) thickness. The values we use for τ and a are 62.8 Myr and 125 km (McKenzie 1978).

The two unknown parameters required to solve eq. (5) are an estimate of the lithosphere stretching factor, β, and the lithosphere thermal equilibration time, t. In oceanic lithosphere, $\beta = \infty$, so the magnitude of the anomaly is only dependent on t, which is the age of the lithosphere and readily obtained from ocean isochrons (e.g. Müller *et al.* 1997).

In continental margin lithosphere, $\beta = tl_0/tl_r$ where tl_0 is thermal equilibrium lithosphere thickness and tl_r is the immediately post-rift lithosphere thickness (McKenzie 1978). The lithosphere thermal equilibration time t is the breakup age at the margin of interest; therefore, the magnitude of the thermal anomaly is dependent on both β and t. In order to estimate β in continental lithosphere, we assume that lithosphere stretching is equal to crustal stretching (i.e. pure shear) and that decompression melting occurs during rifting making a magmatic addition to the stretched continental crust where β exceeds β_{crit}, the stretching factor at which decompression of the upwelling mantle is sufficient to generate melt.

$$\beta = tc_0/tc_{\text{now}} \quad 1 < \beta < \beta_{\text{crit}} \quad (6)$$

$$\beta = tc_0/\left(tc_{\text{now}} - tc_{\text{mag}}\right) \quad \beta > \beta_{\text{crit}} \quad (7)$$

in which tc_0 is the pre-stretching continental crustal thickness; tc_{now} is total present day crustal thickness and tc_{mag} is the thickness of magmatic addition to the crust. The decompression-melting model of McKenzie & Bickle (1988) allows us to estimate β_{crit} as a function of mantle potential temperature (Figs 3a and b). We estimate the appropriate melt addition parametrization using seismic observations of oceanic crustal thickness at the OCT and the decompression

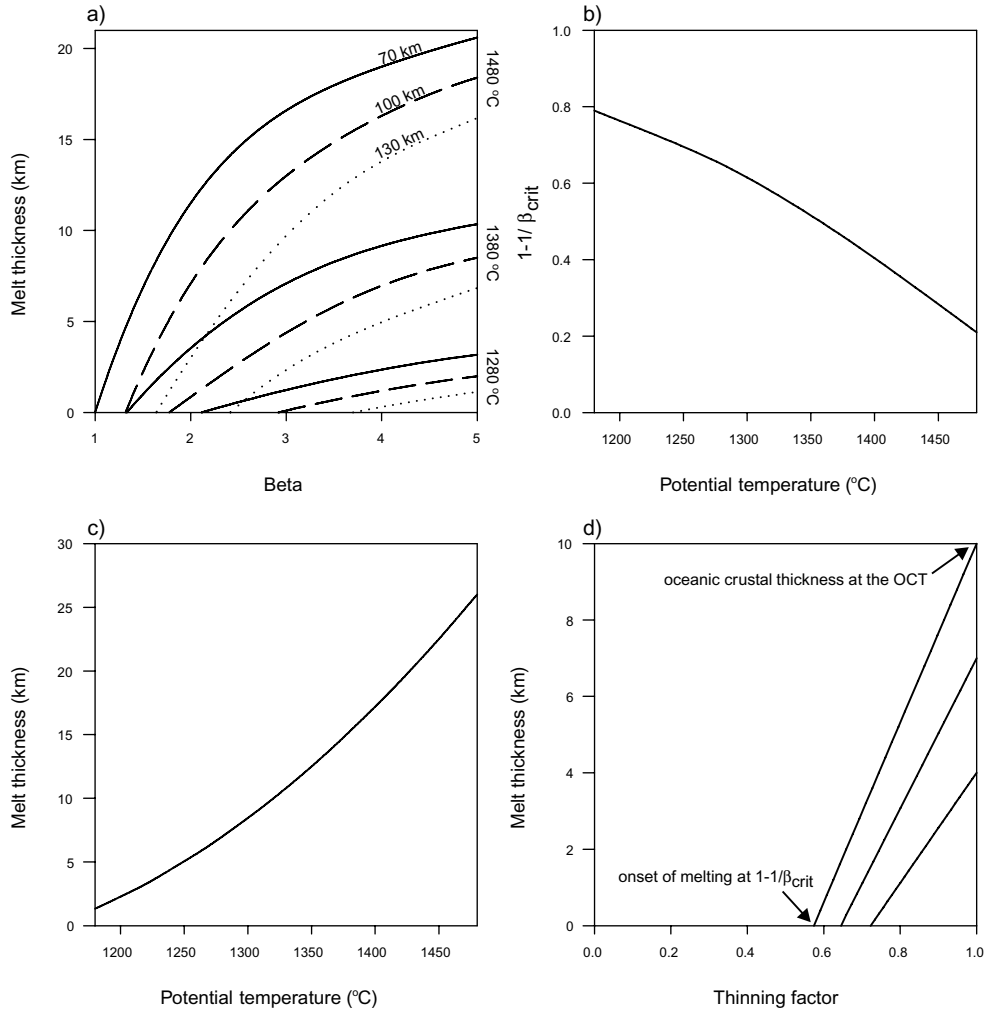

Figure 3. (a) Melt thickness as a function of β stretching factor for mantle potential temperatures of 1280, 1380 and 1480 °C, for mechanical lithosphere thicknesses of 70, 100 and 130 km (redrawn from McKenzie & Bickle 1988). (b) The relationship between β_{crit} for the onset of melting and mantle potential temperature for 100 km mechanical lithosphere thickness. (c) The relationship between melt thickness, or oceanic crustal thickness, and mantle potential temperature at $\beta = \infty$ (White & McKenzie 1989). (d) Interpolated melt thickness as a function of lithosphere thinning factor between melt onset at the critical thinning factor β_{crit} at the associated potential temperature and the observed oceanic crustal thickness at the OCT.

melting model of White & McKenzie (1989) (Fig. 3c). We then find the thickness of magmatic addition as a function of lithosphere thinning factor $[1-(1/\beta)]$ by interpolating between the lithosphere thinning factor for the onset of melt $[1-(1/\beta_{\rm crit})]$, at which $tc_{\rm mag}=0$, and a lithosphere thinning factor of 1, representing oceanic lithosphere, at which $tc_{\rm mag}=tc_{\rm now}$ (Fig. 3d).

We calculate temperature anomaly on a grid with 5 km vertical and lateral spacing using eq. (5) and then, from the temperature anomaly, the associated density anomaly using

$$\Delta\rho=-\alpha\rho\Delta T, \tag{8}$$

in which the thermal expansion coefficient $\alpha=3.28\times10^{-5}K^{-1}$. We assume that each horizontal layer of the grid represents a 5 km thick layer and calculate the lithosphere thermal gravity anomaly of each layer using upward continuation of the anomaly to the surface. We then sum the anomalies calculated for each layer to get the total lithosphere thermal gravity anomaly.

We show the effect of the lithosphere thermal gravity anomaly correction on the Moho depth prediction from the gravity inversion in Fig. 4. For this profile across the North Atlantic, the inversion with the correction is in good agreement with the seismic Moho depth estimates, apart from in the Hatton Basin (1400–1550 km) where the omission of a correction for several kilometres of sediment increases Moho depth. In contrast, the gravity inversion without the correction predicts Moho depth which is a poor fit at the continental margins and is ∼15 km too deep at the ocean ridge.

In the determination of the lithosphere thermal gravity anomaly, we assume a much-simplified model of rifted continental margin formation and structure. Recent observations of depth dependent lithosphere stretching (Driscoll & Karner 1998; Davis & Kusznir 2004; Kusznir & Karner 2007) and exhumed mantle (Pickup *et al.* 1996) at continental margins are not compatible with a pure shear lithosphere thermal model and a continuous increase in melt thickness with stretching magnitude. The specific errors from these assumptions are difficult to quantify; however, we show the effect on the lithosphere thermal gravity anomaly of wrongly estimating the thinning factor in the continental margin lithosphere and of using a cooling-plate model which assumes 1-D cooling (McKenzie 1978). We illustrate this with a number of generalized sensitivity tests that which are typical of those necessary to determine a best fitting model in practice.

2.2.1 Testing the 1-D cooling assumption

At rifted continental margins, cool unthinned continental lithosphere exists close to hot oceanic lithosphere at the same depth, causing a lateral temperature gradient and heat flow from oceanic to continental lithosphere. By using a cooling-plate model which omits lateral heat-transfer, we may be underestimating the temperature of the rifted margin continental lithosphere and overestimating the temperature of the adjacent oceanic lithosphere. Differences in the lithosphere thermal gravity anomaly and Moho depth predictions are evident at the continental margins when we substitute a comparable 3-D thermal model which incorporates lateral heat transfer for the cooling plate model calculated with eq. (5). In Fig. 5, we see these differences on the Hatton Bank margin where the 1-D model predicts a shallower oceanic Moho and a deeper continental Moho. The differences in predicted Moho depth between the 1-D and 3-D thermal models arise due to a combination of the change in lithosphere thermal gravity anomaly and the associated change in predicted thinning factor. An interdependence of the thinning factor and lithosphere thermal gravity estimate occurs in the gravity inversion scheme (Fig. 2) because changing the magnitude of the lithosphere thermal gravity anomaly feeds back into the thinning factor estimate. In order to investigate whether the assumption of 1-D cooling at rifted continental margins adversely affects the predicted magnitude of the lithosphere thermal gravity anomaly, we must therefore, remove the effect of changes in thinning factor to isolate the difference in the lithosphere thermal gravity anomaly that exists between the 1-D and 3-D models.

We investigate the maximum error in the lithosphere thermal gravity anomaly caused by assuming 1-D cooling, by constructing comparable synthetic 1-D and 2-D thermal models representing sections through a margin with an abrupt change in thinning factor from zero to oceanic values (Fig. 6) and a slow spreading rate. This geometry will create the maximum possible lateral temperature gradient and is, therefore, a worst-case scenario. In all models, we specify the thinning factor so that we are only looking at the difference due to the assumption of 1-D cooling.

The 2-D numerical models are calculated using explicit finite-differences and use the same plate-thickness, thermal parameters and boundary conditions as the McKenzie (1978) cooling plate model. At the edges of the model, we specify $\mathrm{d}T/\mathrm{d}y=0$ to minimize edge effects. We assume instantaneous thinning and calculate temperatures on a 2-D grid with 5 km vertical and horizontal spacing. We calculate the lithosphere thermal gravity anomaly in exactly the same way as for the 1-D case described in Section 2.2.

Initially, the 1-D and 2-D models are identical since we base them on the same initial perturbation of lithosphere thickness. Fig. 6 shows that at 5 Myr the 1-D lithosphere model contains a short wavelength ∼10 mGal underestimate of the lithosphere thermal gravity anomaly in the continental margin lithosphere due to the lack of lateral heat transfer from the nearby ocean ridge. As time progresses the magnitude of the underestimate diminishes and a corresponding overestimate of the lithosphere thermal gravity develops in the marginal oceanic lithosphere. The wavelength of the difference between the 1-D and 2-D models increases with time reflecting the increasing depth of the maximum temperature anomaly and lateral heat transfer in the 2-D model. Where we see short (<150 km) wavelength differences, the low-pass filter we apply in the gravity inversion may additionally reduce the magnitude of the error we induce by using the 1-D cooling plate model. In the models we show in Fig. 7, we represent a wider margin, with the change in thinning factor from 0 to 1 taking place over 100 km. Increasing the width of the margin results in differences between the 1-D and 2-D models which are smaller in magnitude and longer in wavelength than the abrupt margin model (Fig. 6). Overall, the potential errors from assuming 1-D cooling are small if eqs (6) and (7) recover the thinning factor correctly.

2.3 Errors in *a priori* OCT location and breakup age

In the method we have described so far, we have assumed that the OCT is accurately located in the plate reconstruction model used to generate the isochrons that determine the lithosphere thermal equilibration time. Unfortunately, plate reconstruction models often generate overlaps to account for the extension at rifted continental margins, with the consequence that the oldest ocean isochrons lie over continental lithosphere. If we know that the isochron age at which seafloor spreading initiated and that its age and location are correct, we can set the OCT to lie at this isochron; however, at some margins, particularly non-volcanic margins, there is no consensus on identifying the oldest seafloor spreading anomalies (e.g. Chalmers

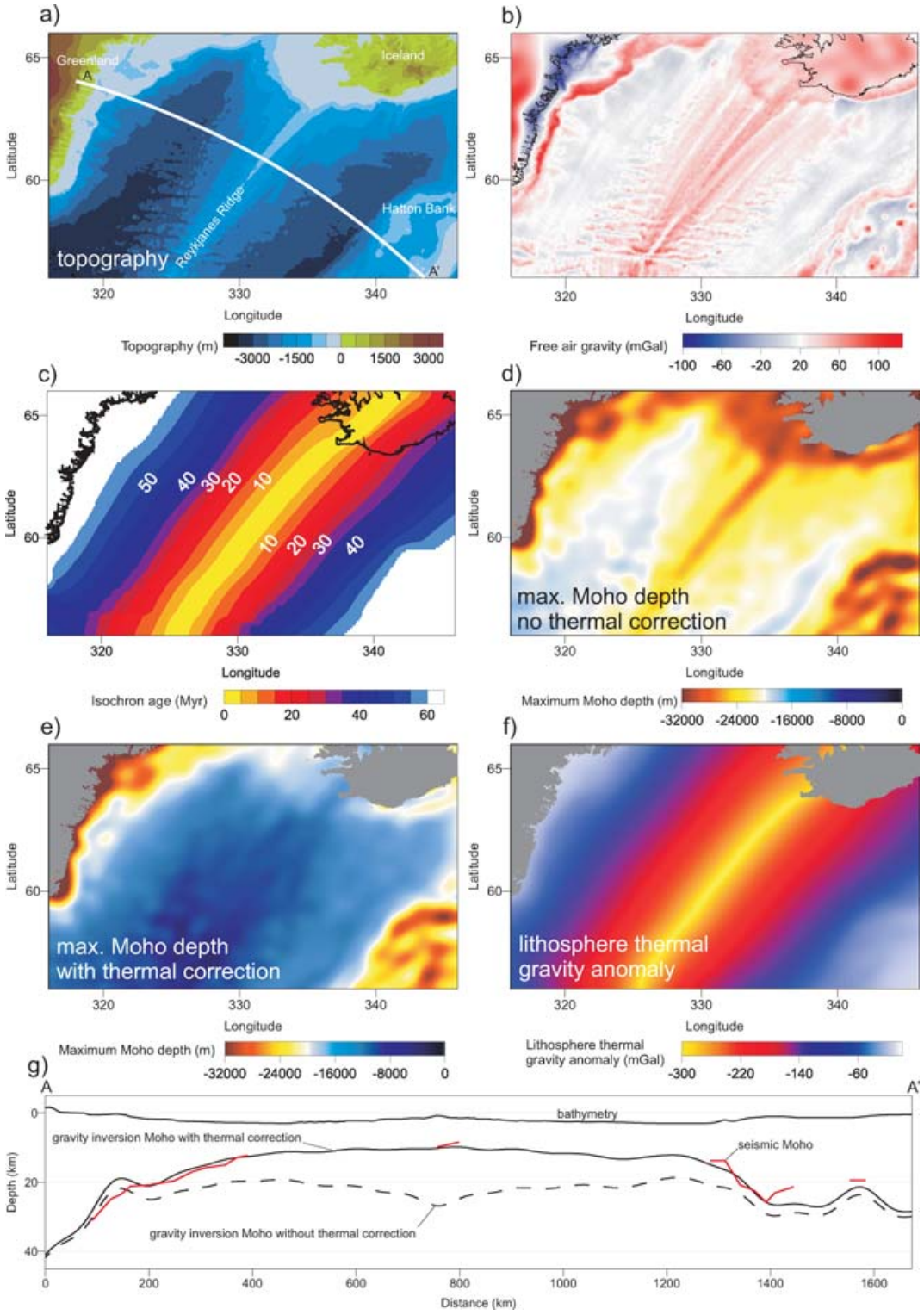

Figure 4. (a) North Atlantic bathymetry showing the location of line A–A′. (b) Free air gravity anomaly (Sandwell & Smith 1997). (c) Ocean isochron ages (Müller *et al.* 1997). (d) Predicted Moho depth from a gravity inversion using no lithosphere thermal gravity anomaly correction. (e) Predicted Moho depth from an otherwise identical gravity inversion incorporating the lithosphere thermal gravity anomaly correction. (f) The lithosphere thermal gravity anomaly resulting from the gravity inversion. (g) Cross-section along line A–A′ comparing Moho depths from gravity inversions with and without the lithosphere thermal gravity anomaly correction (solid and dashed black lines, respectively). Seismic estimates of Moho depth (Morgan *et al.* 1989; Smallwood & White 1998; Hopper *et al.* 2003; Smith *et al.* 2005) from close to line A–A′ are also shown (red line). Moho depth predictions from the gravity inversion including the lithosphere thermal gravity anomaly correction are consistent with seismic estimates, while Moho depth predicted by gravity inversion excluding the thermal gravity anomaly correction are too deep. No correction for sediment thickness has been made. A reference crustal thickness of 32 km has been used.

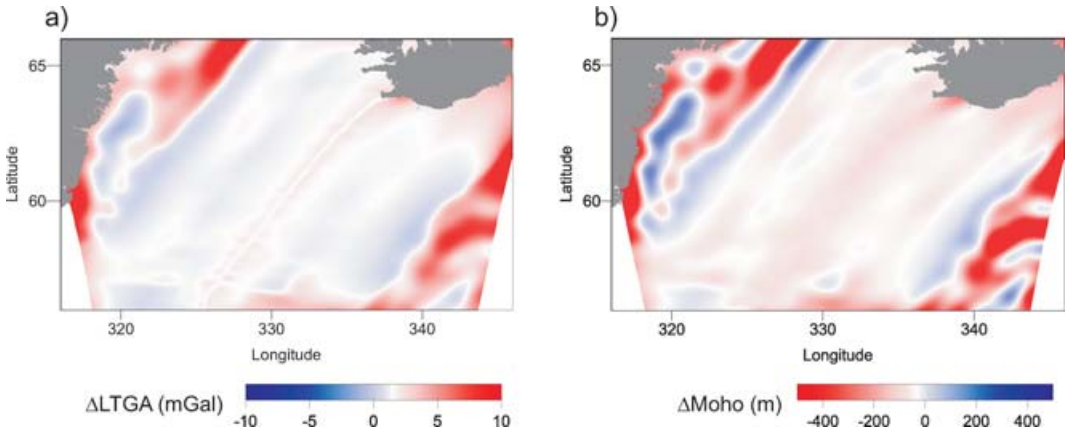

Figure 5. (a) The difference in predicted lithosphere thermal gravity anomaly (1-D–3-D) between an inversion using the 1-D cooling plate model (McKenzie 1978) and an otherwise identical inversion which uses a 3-D numerical cooling model showing the effect of lateral heat transfer. In the ocean centre the difference between the 1-D and 3-D models are negligible. In oceanic lithosphere adjacent to the rifted margins, the 1-D model is hotter than the 3-D model because of the lack of lateral heat transfer, producing a greater lithosphere thermal gravity anomaly and negative values of ΔLTGA. In continental margin lithosphere the 1-D model is correspondingly cooler than the 3-D model and has positive values of ΔLTGA. This relationship is clearest at the Hatton Bank margin. The Greenland margin has a more complex structure and predicted thinning factors are perturbed by the glacio-marine sediment fan at the shelf break. (b) The difference in predicted Moho depth between an inversion using the 1-D cooling plate model (McKenzie 1978) and an otherwise identical inversion using a 3-D numerical cooling model (1-D–3-D). Where ΔLTGA is negative a corresponding positive value of ΔMoho (1-D–3-D) exists.

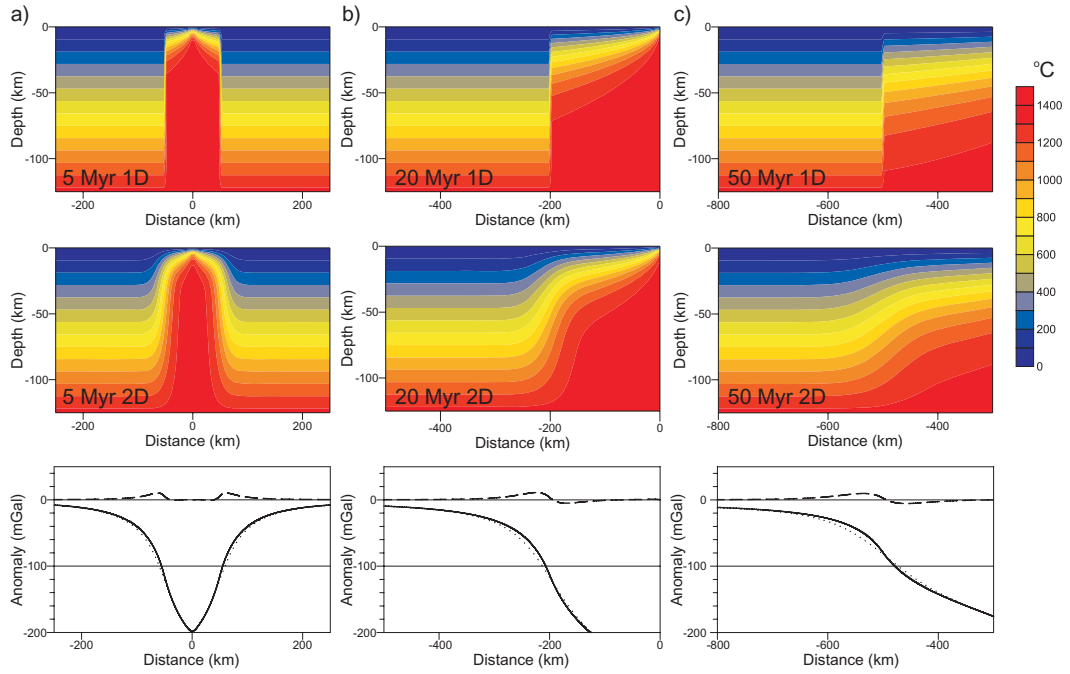

Figure 6. Temperature field and corresponding lithosphere thermal gravity anomalies predicted for a hypothetical ocean basin lithosphere model opening at 1 cm a^{-1} with abrupt rifted margins where thinning factor $[1 - (1/\beta)]$ jumps from 0 to 1.0 (oceanic lithosphere) over a short distance (<5 km). (a) Temperature field calculated at 5 Myr using the 1-D cooling plate model (McKenzie 1978); temperature field calculated at 5 Myr using the 2-D finite-difference scheme described in the text; lithosphere thermal gravity anomalies calculated from the 1-D (solid line) and 2-D (dotted line) models, and the difference (2-D-1-D) between the models (dashed line). (b) As above but at 20 Myr. (c) As above at 50 Myr. The abrupt transition from continental to oceanic lithosphere gives the greatest lateral temperature gradients possible and, therefore, the greatest difference between a 1-D cooling-plate lithosphere model and a 2-D model incorporating lateral heat transfer.

& Laursen 1995; Russell & Whitmarsh 2003; Tucholke *et al.* 2007) so this approach often not possible.

We consider a number of ways of defining the OCT for the purpose of the gravity inversion using examples from the Hatton Bank margin (Fig. 8a), because of its relatively simple geometry and well-defined OCT. The margin is largely sediment starved and there are seismic estimates of oceanic crustal thickness (∼12 km) and OCT location (Morgan *et al.* 1989). Breakup age is ∼55 Ma (Doré *et al.* 1999). In the Müller *et al.* (1997) data set, the location of the breakup age (55 Ma) isochron corresponds to the observed OCT location (Morgan *et al.* 1989). However, the isochrons data set incorrectly places the breakup at an age of ∼60 Myr and the OCT 45 km further

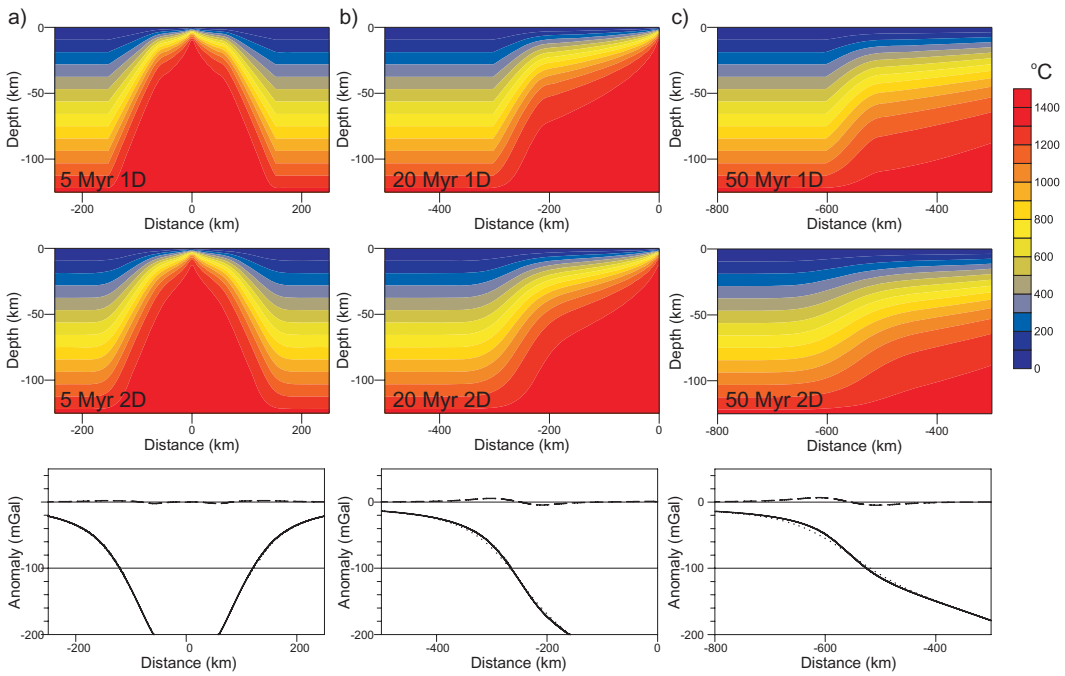

Figure 7. Temperature field and corresponding lithosphere thermal gravity anomalies predicted for a hypothetical ocean basin lithosphere model opening at 1 cm a^{-1} with rifted margins at which thinning factor $[1 - (1/\beta)]$ increases from 0 to 1.0 (oceanic lithosphere) over 100 km. Description otherwise as for Fig. 6. A lithosphere thinning transition width of 100 km is still a narrow margin and differences in the lithosphere thermal gravity anomaly between 1-D and 2-D models are substantially smaller than the abrupt model (Fig. 6). Errors in the lithosphere thermal gravity anomaly due to the assumption of 1-D rather than 2-D cooling are small.

into the continental margin. We condition the melt correction of the thinning factor using 12 km as oceanic crustal thickness; the associated potential temperature of ∼1340 °C (Fig. 3c) gives $1 - (1/\beta_{crit}) = 0.54$ (Fig. 3b). Fig. 8(b) shows a model in which we prescribe the OCT at the 55 Ma isochron which is at the correct OCT location based on the *a priori* information. We now compare this model with other approaches to defining the OCT location to investigate the effect of errors in the OCT location on Moho depth and thinning factor predictions, which may arise when we have incomplete or inaccurate information (Fig. 8).

In Fig. 8(c) we have used the full range of the isochrons in the Müller *et al.* (1997) data set (0–60 Ma) to define oceanic lithosphere (thinning factor = 1) and used the implied 60 Ma breakup age in the continental margin. The Moho depth prediction is up to 1 km shallower than the model using *a priori* data (Fig. 8b) in the continental margin. The thinning factor of ∼0.3 at the OCT is inconsistent with the predicted value for the onset of melt, $1-(1/\beta_{crit}) = 0.54$. In Fig. 8(d), we place the OCT at the 45 Ma isochron and use the correct 55 Ma breakup age. The Moho depth prediction is <300 m deeper than the model using *a priori* data (Fig. 8b) in the oldest oceanic lithosphere. This is because eq. (7) largely recovers the oceanic thinning factor in the region between the 45 and 55 Ma isochrons. In Fig. 8(e), we make no assumption of the OCT location and use the 55 Ma breakup age throughout. The Moho depth prediction is <1 km deeper than the model using *a priori* data (Fig. 8b) in the continental margin and reaches ∼2 km deeper at the end of the section (∼37 Ma). The location of the OCT is displaced slightly oceanwards and the thinning factors at greater than 150 km are <1 due to the overestimated cooling age causing an underestimate of the lithosphere thermal gravity anomaly in the younger oceanic lithosphere. The reduction in magnitude of the long-wavelength components of the lithosphere thermal gravity anomaly slightly reduces thinning factors in the continental margin. In Fig. 8(f), we define oceanic lithosphere as being where the gravity inversion predicts a thinning factor of 1. In oceanic lithosphere where the isochron age is <55 Ma we use the isochron age and where the isochron age is ≥55 Ma we use 55 Ma. Breakup age in continental lithosphere is 55 Ma. The differences in Moho depth between this model and the model using *a priori* data are negligible and the difference in thinning factor is also small.

From this example we can see that the differences between the reference model (Fig. 8b) and the models using assumptions in locating the OCT (Figs 8c–f) are generally small at the continental margin when we include predicted melt addition in the determination of the thinning factor (eq. 7). Small errors in isochron age have negligible effect (compare Figs 8d and f). The largest differences occur when we misplace the OCT into the continental lithosphere (Fig. 8c) which suggests that our modelling approach should always be to try to avoid this situation by omitting the oldest isochrons (Figs 8d–f).

In using this example, a 'middle-aged' margin of a wide ocean basin, we are seeing a negligible dependence on errors in OCT location and age which have little effect on the width of the basin; however, in young, narrow ocean basins, we see strong dependence on these variables. To demonstrate the effect of typical OCT location and age errors on the lithosphere thermal gravity anomaly at different times in a basins history, we perturb the synthetic model introduced in Fig. 6.

In Fig. 9(a), we show the ocean basin at 5 Myr after breakup with the OCT correctly located. In Fig. 9(b), the OCT is mislocated 25 km into the continental margin and we assume that a corresponding extra 2.5 Myr of seafloor spreading has taken place. In the 25 km interval between the true OCT and the assumed location, we prescribe oceanic thinning factors. This results in the marginal

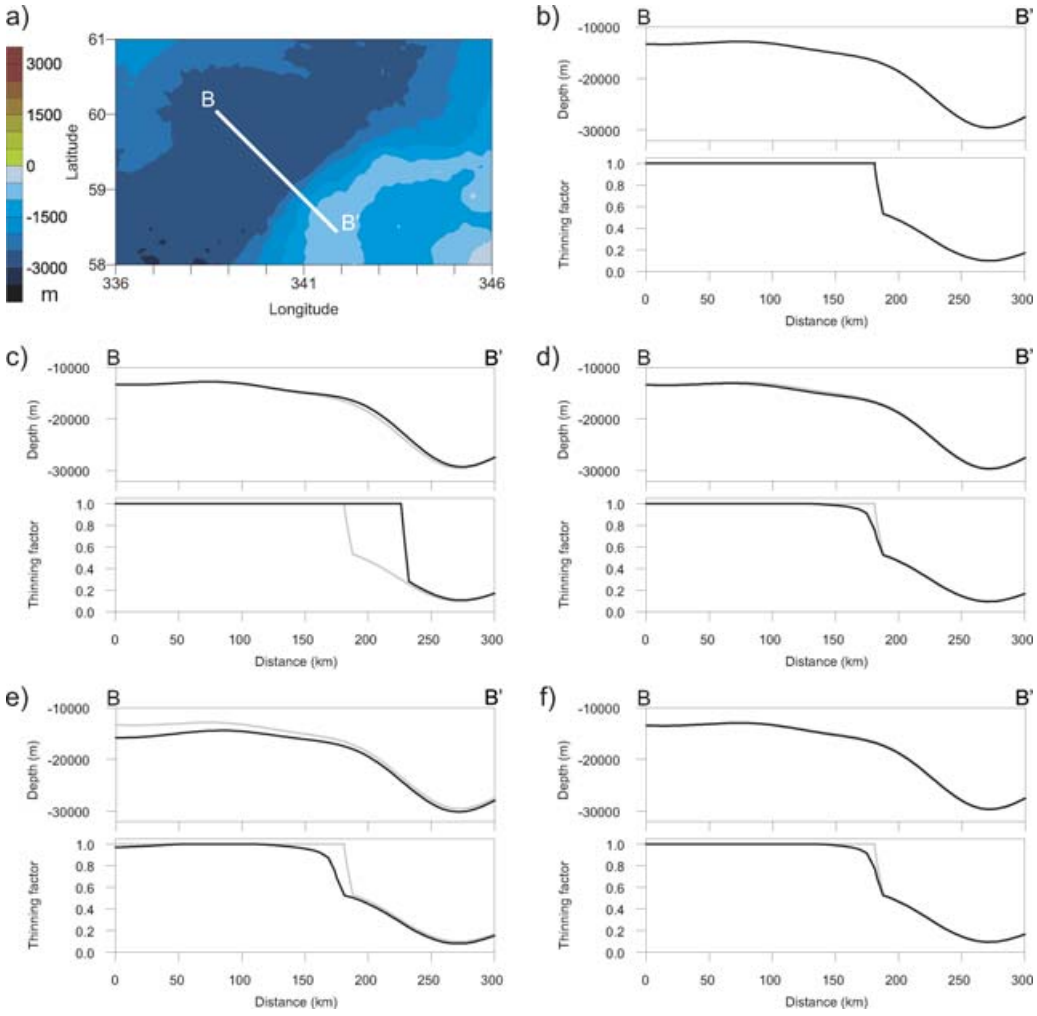

Figure 8. (a) Location of the section B–B′ across the Hatton Bank rifted margin used to illustrate different ways of conditioning the lithosphere thermal model used to determine the lithosphere thermal gravity anomaly correction. (b) Moho depth and thinning factor prediction from the reference model using all of the *a priori* information [breakup age = 55 Ma) to define the OCT (shown in grey throughout (c–f)]; (c) using the full extent of isochrons and the oldest isochron age (60 Ma) as breakup age; (d) using the 45 Ma isochron as the oldest prescribed oceanic lithosphere and 55 Ma break up age everywhere else; (e) using 55 Ma break up age and the melt-corrected thinning factor throughout; (f) using isochron age up to 55 Ma where the melt-corrected thinning factor predicts oceanic lithosphere and 55 Ma otherwise.

lithosphere prediction being significantly hotter when the OCT is mislocated in the thermal model. Fig. 9(c) shows the error in lithosphere thermal gravity anomaly resulting from the OCT mislocation. At the margin, the error is ∼70 mGal and at the ocean ridge it is ∼30 mGal. In this narrow basin (100 km) the lithosphere thermal gravity anomaly magnitude is suppressed by the upward continuation effect since the wavelength of the anomaly is short in relation to the thickness of the lithosphere. In this context, 50 km total error (25 km at each margin) increases the width of the basin by 50 per cent and the wavelength of the anomaly by a similar length, thereby considerably reducing the suppression due to upward continuation. At 20 and 50 Myr this effect is much smaller, causing negligible changes in magnitude at the ocean ridge since the basin is much wider. For these older models, the local errors at the continental margin remain non-negligible at ∼20 and ∼10 mGal, respectively.

In Fig. 9(d), we show the same ocean basin at 5 Myr with the OCT correctly located. In Fig. 9(e), the OCT is mislocated 25 km into the ocean and we assume that there has correspondingly been 2.5 Myr less seafloor spreading. In the 25 km between the true OCT and the assumed location, we solve for thinning factor. Fig. 9(f) shows that at 5 Myr the error in the lithosphere thermal gravity anomaly is < -7 mGal which is due to the error in the age of the 25 km of oceanic crust between the true and assumed OCT locations. If the oceanic thinning factor is recovered correctly by eq. (7), the width of the basin is unaffected and the large continuation effects seen with the opposite error polarity (Fig. 9c) do not exist. Errors are negligible for the model at 20 and 50 Myr.

For young ocean basins and rifted margins, it appears that prescribing the OCT location incorrectly by a few tens of kilometres creates several kilometres of systematic error in predicted Moho depth. In these circumstances, the safest approach is probably to predict the OCT with the melt corrected thinning factor, either omitting the oldest isochrons (as described for Figs 8a and f) or using a constant thermal re-equilibration age corresponding to breakup (Fig. 8e). In contrast, the errors in the lithosphere thermal gravity anomaly caused by errors in age, due to mislocating the OCT oceanwards, are an order of magnitude smaller and in many situations, it may be better to allow these small errors, rather than risk the large errors from having the OCT located too far continentwards.

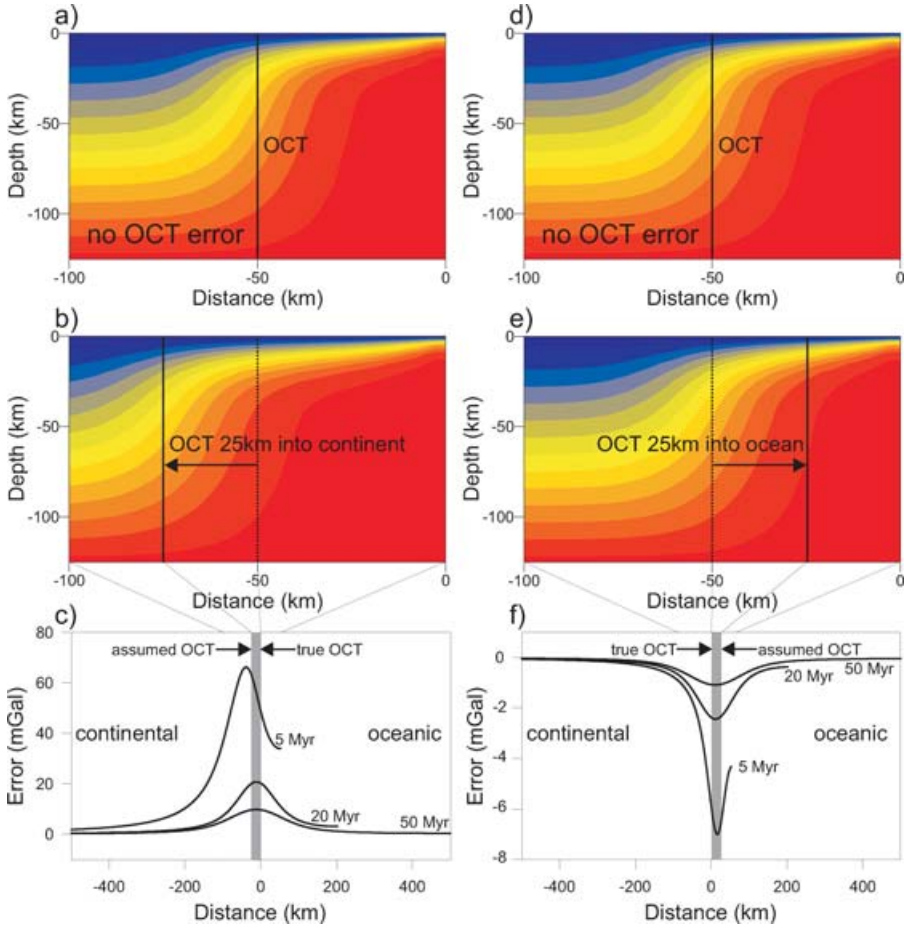

Figure 9. Sensitivity of lithosphere thermal gravity anomaly correction to OCT location. (a) Temperature field of a hypothetical ocean basin lithosphere model after 5 Myr of seafloor spreading at 1 cm a^{-1} with abrupt margins at which thinning factor $[1 - (1/\beta)]$ jumps from 0 to 1.0 over a short distance (<5 km). (b) As in (a); however, in this case, the OCT is mislocated in error by 25 km towards the continent and has an age of 7.5 Ma representing a worst case scenario for 25 km error since the margin is abrupt and the spreading rate low. (c) The difference in lithosphere thermal gravity anomaly (true OCT model—erroneous OCT model) at 5, 20 and 50 Myr for 25 km OCT error towards the continent. (d) As for (a). (e) As in (a); however, in this case the OCT is mislocated in error by 25 km towards the ocean and has an age of 2.5 Ma. (f) The difference in lithosphere thermal gravity anomaly (true OCT model—erroneous OCT model) at 5, 20 and 50 Myr for 25 km OCT error towards the ocean. For the same OCT error the difference in lithosphere thermal gravity anomaly is an order of magnitude smaller when the OCT is mislocated in error towards the ocean.

In Fig. 10(a), we show again the ocean basin at 5 Myr for which we have calculated the temperature field using a thermal model conditioned by isochron ages derived from the assumed spreading rate of 1 cm a^{-1}. In Fig. 10(b), we show the basin at 5 Myr with the temperature calculated using the breakup age throughout. This will give the correct equilibration age in the continental margin; however, in oceanic lithosphere it will overestimate equilibration age by an increasing amount towards the ocean ridge. Consequently, the predicted oceanic lithosphere temperature is lower, leading to an underestimate of the lithosphere thermal gravity anomaly magnitude; however, this only has a small effect in the continental margin lithosphere. There is little difference in the continental margin thermal structure and the small difference in lithosphere thermal gravity anomaly arises from the underestimated long-wavelength component from the adjacent oceanic lithosphere. In the continental margin lithosphere the error in the predicted lithosphere thermal gravity anomaly between models using breakup age throughout and models using isochrons in oceanic lithosphere remains small as age increases (Fig. 10c). Hence, if we are only interested in predicting OCT location and Moho depth in continental margin lithosphere and ocean isochrons are unavailable or incorrect, we can use an estimate of breakup age to condition the thermal model in the gravity inversion.

3 DISCUSSION

The method described in this paper uses a simple earth model (water, sediment, crust and mantle) and standard lithosphere thermal models to invert gravity anomalies for Moho depth at rifted continental margins. This leads us to consider the limitations of the method. In particular, we cannot calibrate the inversion or interpret results where our assumed earth model or thermal model assumptions are not valid, as the results will contain systematic errors. For example, if we were to extend inversion from the Hatton Bank margin (Fig. 4), where breakup is in the late Palaeocene and is characterized by thick oceanic crust, into the Rockall Trough and Goban Spur margins to the southeast, in which rifting and breakup are early Cretaceous and characterized by thin oceanic crust, we should not interpret the results in the latter if we had conditioned the thermal model with break up age and melt addition correction appropriate to the Hatton Bank margin. This may require using a separate model conditioned

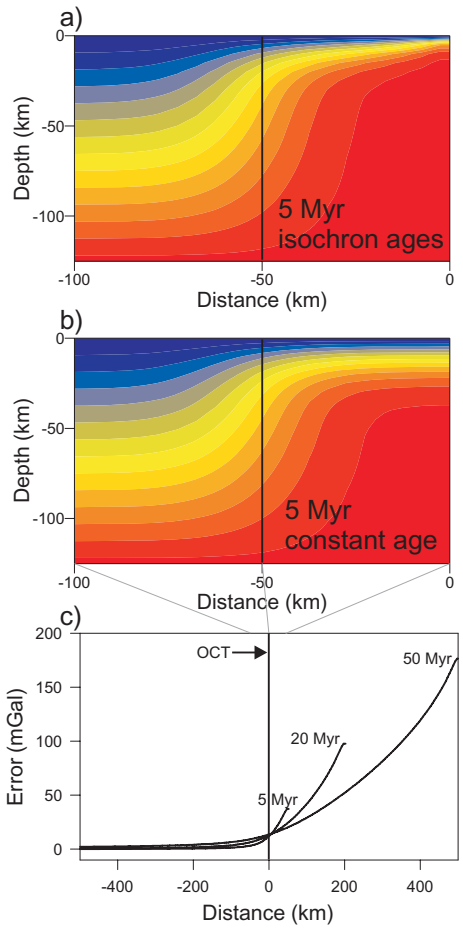

Figure 10. Sensitivity of lithosphere thermal gravity anomaly correction to error in breakup age. (a) Temperature field of a hypothetical ocean basin lithosphere model after 5 Myr of seafloor spreading at 1 cm a^{-1} with abrupt rifted margins at which thinning factor $[1 - (1/\beta)]$ jumps from 0 to 1.0 over a short distance (<5 km). (b) As in (a) apart from a constant thermal perturbation age (0 Myr) being used throughout the model. At the ocean ridge (0 km) the constant age model overestimates the lithosphere equilibration time and temperature is underestimated. Towards the continental margin the difference between (a) and (b) becomes smaller. Panel (c) shows the error in lithosphere thermal gravity anomaly magnitude between models using isochron ages in oceanic lithosphere and those using constant thermal perturbation ages of 5, 20 and 50 Myr. Errors in the lithosphere thermal gravity anomaly for continental margin lithosphere are negligible and have little effect on the predicted OCT location.

with an appropriate breakup age and oceanic crustal thickness for each margin segment.

Equally important is how we vary reference crustal thickness to try to match predicted Moho depths to seismic observations. These will only correspond where our earth model is a good approximation to the lithosphere structure. At volcanic rifted margins this is problematic since anomalously thick oceanic crust produced at elevated mantle potential temperatures invariably has a higher than average density (White & McKenzie 1989). The gravity predicted Moho will be shallower than the seismic Moho in this case because of the standard density contrast between crust and mantle used in the inversion will be too large. At non-volcanic margins calibration is equally difficult since the seismic Moho ($V_p > 8$ km s^{-1}) does not represent the petrological crust–mantle interface. In this case, the predicted Moho would be expected to lie somewhere close to the base of the superficial crust or serpentinized mantle layer, since this is likely to have a density close to our assumption of crustal density, and the associated high seismic velocity lower crust has a density close to upper mantle density.

The most reliable calibrations are where well-constrained wide-angle seismology gives Moho depth in magmatic oceanic crust <10 km thickness or in failed breakup basins, where the structure matches our earth model (water, sediment, crust and mantle). At regional scale, reference crustal thickness is remarkably constant and our experience suggests that locally large variations (>1 km) are more likely to result from an inaccurate earth or thermal model.

The accuracy of the lithosphere thermal gravity anomaly is critical to producing accurate Moho depth predictions at rifted continental margins because of the large magnitude of the thermal gravity anomaly. This depends on the accuracy of the thermal model and the accuracy of the parameters we use to condition it. In oceanic lithosphere, the thermal mass deficiency is responsible for both the subsidence of the lithosphere as it cools and the lithosphere thermal gravity anomaly. In the plate model that we utilize (McKenzie 1978), the parameters have been derived by inverting the observed increase in bathymetry with age (Parsons & Sclater 1977) thereby calibrating the change in mass deficiency. By using this model, the integral of the lithosphere mass deficiency is calibrated. However, in using constant diffusivity and plate thickness constrained by inversion of the isostatic subsidence model, the cooling plate model produces an arbitrary representation of the geotherm and limited control on the depth distribution of the mass deficiency. Because of upward continuation, the lithosphere thermal gravity anomaly is of course sensitive to the depth of the mass deficiency. More complex representations of the oceanic geotherm (Hofmeister 1999; McKenzie *et al.* 2005), those utilizing more extensive observations (e.g. Stein & Stein 1992) and seismic estimates of lithosphere thickness (e.g. Ritzwoller *et al.* 2004; Maggi *et al.* 2006) suggest that the earlier models probably overestimate the thickness of the oceanic lithosphere. By using the McKenzie (1978) lithosphere model, we are likely to be underestimating the lithosphere thermal gravity anomaly.

If we take care not to prescribe oceanic thinning factors in continental margin lithosphere by using inaccurate ocean isochrons, then conditioning the thermal model to produce a reasonable lithosphere thermal gravity anomaly at a continental margin is straightforward. Apart from in young ocean basins, the predicted lithosphere thermal gravity anomaly is generally more sensitive to thinning factor than age in the continental margin lithosphere (Chappell & Kusznir 2008a). This allows us to use melt-corrected thinning factors to predict OCT location, thus reducing the reliance on the isochron data. Any oceanic isochron distribution embodies a particular plate reconstruction model and that often includes simplification and errors in the margin geometry and breakup age. At breakup age, at many margins, there is no consensus amongst existing plate models, so using the oldest isochrons derived from these models requires considerable caution.

4 CONCLUSIONS

We have shown that it is possible to calculate iteratively a deterministic estimate of the gravity anomaly caused by lateral changes in lithosphere temperature and density at rifted continental margins, as part of a scheme for determining Moho depth by gravity inversion.

This is necessary to predict Moho depth in rifted continental margin and oceanic lithosphere.

The errors introduced into the calculation of the lithosphere thermal gravity anomaly at rifted continental margins by using a fast analytic 1-D cooling plate model to approximate a more realistic, but computationally slower, 3-D model of the lithosphere temperature field are small.

Using an inaccurate definition of the OCT location and age (e.g. by using inaccurate oceanic isochrons) can potentially lead to large errors in the lithosphere thermal gravity anomaly and predicted Moho depth at rifted margins particularly for young, narrow ocean basins. The extent of ocean isochrons used to define oceanic lithosphere location and age, used to condition the lithosphere thermal model in the gravity inversion, can be adjusted to avoid these errors. These strategies allow us to use the gravity inversion to determine rifted margin Moho depth and OCT location where age or location of the OCT are not well understood.

ACKNOWLEDGMENTS

This work was supported by a PhD studentship awarded to A.R. Chappell by the NERC Margins iSIMM project, funded by the DTI, AGIP UK (ENI UK), BP, Amerada Hess, Anadarko, ConocoPhillips, Shell, Statoil and Western Geco.

REFERENCES

Bott, M.H.P., 1960. The use of rapid digital computing methods for direct gravity interpretation of sedimentary basins, *Geophys. J.R. astr. Soc.,* **3,** 63–7.

Breivik, A.J., Verhoef, J. & Fáleide, J.I., 1999. Effect of thermal contrast on gravity modelling at passive margins: Results from the western Barents Sea, *J. geophys. Res.,* **104,** 15 293–15 311.

Carlson, R.L. & Herrick, C.N., 1990. Densities and porosities in the oceanic crust and their variations with depth and age, *J. geophys. Res.,* **95,** 9153–9170.

Chalmers, J. A. & Laursen, K.H., 1995. Labrador Sea: the extent of continental and oceanic crust and the timing of the onset of sea floor spreading, *Mar. Pet. Geol.,* **12,** 205–217.

Chappell, A.R. & Kusznir, N.J., 2008a. Crustal structure of the Norwegian-Greenland Sea from satellite gravity inversion incorporating a correction for the lithosphere thermal gravity anomaly, in *Proceedings of the Faroe Island Exploration Conference 2006,* Jardfeingi, Torshavn.

Chappell, A.R. & Kusznir, N.J., 2008b. An algorithm to calculate the gravity anomaly of sedimentary basins with exponential density-depth relationships, *Geophys. Prospect.,* **56,** 249–258

Christensen, N.I. & Mooney, W.D., 1995. Seismic velocity structure and composition of the continental crust: a global view, *J. geophys. Res.,* **100,** 9761–9788.

Cochran, J.R. & Talwani, M., 1977. Free-air gravity anomalies in worlds oceans and their relationship to residual elevation. *Geophys J. R. astr. Soc.,* **50,** 495–552.

Cordell, L. & Henderson, R.G., 1968. Iterative three-dimesional solution of gravity anomaly data using a digital computer, *Geophysics,* **33,** 596–601.

Crosby, A.G., McKenzie, D.P. & Sclater, J.G., 2006. The relationship between depth, age and gravity in the oceans, *Geophys. J. Int.* **166,** 553–573.

Davis M. & Kusznir, N.J., 2004. Depth-dependent lithospheric stretching at rifted continental margins, in *Proceedings of the NSF Rifted Margins Theoretical Institute,* pp. 92–136, Columbia University Press, New York.

Doré, A.G., Lundin, E.R., Jensen, L.N., Birkeland, Ø., Eliassen, P.E. & Fichler, C., 1999. Principal tectonic events in the evolution of the northwest European Atlantic margin, in *Petroleum Geology of Northwest Europe: Proceedings of the 5th Conference,* pp. 41–61, The Geological Society, London.

Driscoll, N.W. & Karner, G.D., 1998. Lower crustal extension across the northern Carnarvon basin, Australia: evidence for an eastward dipping detachment, *J. geophys. Res.,* **103,** 4975–4991.

Granser, H., 1986. Convergence of iterative gravity inversion, *Geophysics,* **51,** 1146–1147.

Granser, H., 1987. Nonlinear inversion of gravity data using the Schmidt-Lichtenstein approach. *Geophysics,* **52,** 88–93.

Greenhalgh, E.E. & Kusznir, N.J. 2007. Evidence for thin oceanic crust on the extinct Aegir Ridge, Norwegian Basin, N.E. Atlantic derived from satellite gravity inversion. *Geophys. Res. Lett.,* **34,** L06305, doi:10.1029/2007GL029440.

Hofmeister, A.M., 1999. Mantle values of thermal conductivity and the geotherm from phonon lifetimes, *Science,* **283,** 1699–1706.

Hopper, J.R., Dahl-Jensen, T., Holbrook, W.S., Larsen, H.C., Lizarralde, D., Korenaga, J., Kent, G.M. & Kelemen, P.B., 2003. Structure of the SE Greenland margin from seismic reflection and refraction data: Implications for nascent spreading centre subsidence and asymmetric crustal accretion during North Atlantic opening, *J. geophys. Res.,* **108,** 2269.

IOC, IHO & BODC, 2003. *Centenary Edition of the GEBCO Digital Atlas, published on CD-ROM on behalf of the Intergovernmental Oceanographic Commission and the International Hydrographic Organization as part of the General Bathymetric Chart of the Oceans,* British Oceanographic Data Centre, Liverpool, UK.

Karner, G.D. & Watts, A.B., 1982. On isostasy at an Atlantic-type continental margin. *J. geophys. Res.,* **87,** 2923–2948.

Kimbell, G.S., Gatliff, R.W., Ritchie, J.D., Walker, A.S.D. & Williamson, J.P., 2004. Regional three-dimensional gravity modelling of the NE Atlantic margin, *Basin Res.,* **16,** 259–278.

Kuo, B.Y. & Forsyth D.W., 1989. Gravity anomalies of the ridge-transform system in the South-Atlantic between 31-degrees-S and 34.5-degrees S-upwelling centres and variations in crustal thickness, *Mar. Geophys. Res.* **10,** 205–232.

Kusznir, N.J. & Karner, G.D., 2007. Continental lithospheric thinning and breakup in response to upwelling divergent mantle flow: applications to the Woodlark, Newfoundland and Iberia margins, in *Imaging, Mapping and Modelling Continental Lithosphere Extension and Breakup,* Vol. 282, pp. 389–419, eds G.D. Karner, G. Manatschal & L.M. Pihero, Geological Society of London Special Publications.

Louden, K.E. & Forsyth, D.W., 1976. Thermal conduction across fracture zones and gravitational edge effects, *J. geophys. Res.,* **81,** 4869–4874.

Maggi, A., Debayle, E., Priestley, K. & Barruol, G., 2006. Multimode surface waveform tomography of the Pacific Ocean: a closer look at the lithosphere cooling signature, *Geophys. J. Int.,* **166,** 1384–1397.

McKenzie, D. P., 1978. Some remarks on the development of sedimentary basins, *Earth planet. Sci. Lett.,* **40,** 25–32.

McKenzie, D.P., Jackson, J. & Priestley, K., 2005. Thermal structure of oceanic and continental lithosphere, *Earth planet. Sci. Lett.,* **233,** 337–349.

McKenzie, D.P. & Bickle, M.J., 1988. The volume and composition of melt generated by extension of the lithosphere, *J. Petrol.,* **29,** 625–679.

Morgan, J.V., Barton, P.J. & White, R.S., 1989. The Hatton Bank Volcanic Margin 3. Structure from wide-angle OBS and multichannel seismic refraction profiles, *Geophys. J. Int.,* **98,** 367–384.

Müller, R.D., Roest, W.R., Royer, J.-Y., Gahagan, L.M. & Sclater, J.G., 1997. Digital isochrons of the world's ocean floor, *J. geophys. Res.,* **102,** 3211–3214.

Oldenburg, D.W., 1974. The inversion and interpretation of gravity anomalies, *Geophysics,* **39,** 526–536.

Parker, R.L., 1972. The rapid calculation of potential anomalies, *Geophys J. R. astr. Soc.,* **31,** 447–455.

Parsons, B. & Sclater, J.G., 1977. Analysis of variation of ocean-floor bathymetry and heat-flow with age, *J. geophys. Res.,* **82,** 803–827.

Pickup, C.L.B., Whitmarsh, R.B., Fowler, C.M.R. & Reston, T.J., 1996. Insight into the nature of the ocean-continent transition off West Iberia from a deep multichannel seismic reflection profile, *Geology* **24,** 1079-

Poudjom Djomani, Y.H., O'Reilly, S.Y., Griffin, W.L. & Morgan, P., 2001. The density of the subcontinental lithosphere through time, *Earth planet Sci. Lett.,* **184,** 605–621.

Ritzwoller, M.H., Shapiro, N.M. & Zhong, S.J., 2004. Cooling history of the Pacific lithosphere, *Earth planet Sci. Lett.,* **226,** 69–84.

Russell, S.M. & Whitmarsh, R.B., 2003. Magmatism at the west Iberia non-volcanic rifted continental margin: evidence from analyses of magnetic anomalies, *Geophys. J. Int.,* **154,** 706–730.

Sandwell, D.T. & Smith, W.H.F., 1997. Marine gravity anomaly from Geosat and ERS 1 satellite altimetry, *J. geophys. Res.,* **102,** 10039–10054.

Sclater, J.G. & Christie, P.A.F., 1980. Continental Stretching: an explanation of the post mid-cretaceous subsidence of the central North Sea basin, *J. geophys. Res.,* **85,** 3711–3739.

Sheriff, R.E. & Geldart, L.P., 1999. *Exploration Seismology,* 2nd edn, Cambridge University Press, Cambridge.

Smallwood, J.R. & White, R.S., 1998. Crustal accretion at the Reykjanes Ridge, 61 degrees–62 degrees N, *J. geophys. Res.,* **103,** 5185–5201.

Smith, L.K., White, R.S., Kusznir, N.J. & the iSIMM team, 2005. Structure of the Hatton Basin and the adjacent continental margin, in *Petroleum Geology: North-West Europe and Global Perspectives–Proceedings of the 6th Petroleum Geology Conference,* pp. 947–956, The Geological Society, London.

Smith, R.A., 1961. A uniqueness theorem concerning gravity fields, *Proc. Cambridge Philos. Soc.,* **57,** 865–70.

Stein, C.A. & Stein, S., 1992. A model for the global variation in oceanic depth and heat-flow with lithospheric age, *Nature,* **359,** 123–129.

Tucholke, B.E., Sawyer, D.S. & Sibuet, J.-C., 2007. Breakup of the Newfoundland-Iberia rift, in *Imaging, Mapping and Modelling Continental Lithosphere Extension and Breakup,* Vol. 282, pp. 9–46, eds G.D. Karner, G. Manatschal & L.M. Pihero, Geological Society of London Special Publications.

Watts, A.B. & Fairhead, J.D., 1999. A process-oriented approach to modeling the gravity signature of continental margins, *Leading Edge,* **18,** 258–263.

Watts, A.B., McKenzie, D.P., Parsons, B.E. & Roufosse, M., 1985. The relationship between gravity and bathymetry in the Pacific-Ocean, *Geophys J. R. astr. Soc.,* **83,** 263–298.

White, R.S. & McKenzie, D.P., 1989. Magmatism at rift zones: the generation of volcanic continental margins and flood basalts, *J. geophys. Res.,* **94,** 7685–7729.